

## Theoretical investigation of 1,4-naphthalene dicarboxylic acid based dye-sensitized solar cells (DSSC)

R Rifca<sup>a</sup>, X Mary Josephine<sup>b</sup>, S Mohankumar<sup>c</sup> & V Sathyanarayanamoorthi\*<sup>a</sup>

<sup>a</sup>Department of Physics, PSG College of Arts and Science, Coimbatore 641 014, India

<sup>b</sup>Department of Physics, Nirmala College for Women, Coimbatore 641 018, India

<sup>c</sup>Department of Electronics, PSG College of Arts and Science, Coimbatore 641 014, India

E-mail: sathyanarayanamoorthi@psgcas.ac.in

Received 1 September 2024; accepted (revised) 28 April 2025

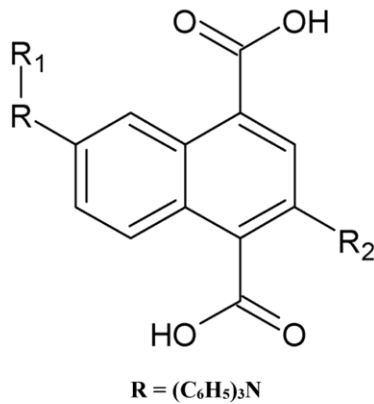
Density Functional Theory (DFT) is used to evaluate the performance of dyes and the role of  $\pi$ -conjugation in dye-sensitized solar cells (DSSCs). This study examines five new 1,4-naphthalene dicarboxylic acid based conjugated donor- $\pi$ -acceptor (D- $\pi$ -A) organic dyes. Each dye features a triphenylamine (TPA) group as the electron donor, while a nitro or cyano group serves as the electron acceptor. Methyl or ethyl groups are used as  $\pi$ -conjugated spacers to investigate the effects of different auxiliary donor groups. DFT calculations with the B3LYP functional and polarized split-valence 6-311+G(d,p) basis sets have been performed to assess excitation energies, absorption spectra, and emission spectra of each dye. The Polarizable Continuum Model (PCM) has been applied to analyze solvent effects. The energy levels of the LUMO and HOMO have been calculated to evaluate their suitability for electron injection and dye regeneration. The HOMO-LUMO gap calculations align well with spectral data. Additionally, the light-harvesting efficiency (LHE), electron injection free energy ( $\Delta G_{\text{inject}}$ ), and oscillator strength ( $f$ ) have been computed and discussed. The study also includes calculations of open-circuit photovoltage ( $V_{\text{oc}}$ ) and electron coupling constant ( $V_{\text{RP}}$ ) for the examined dye-sensitizers.

**Keywords:** 1,4-Naphthalene dicarboxylic acid derivatives, Dye sensitized solar cells, Density functional theory, Light harvesting efficiency

The heavy use of fossil fuels has led to their depletion and contributed to environmental pollution and the greenhouse effect. To address these issues, the commercialization of renewable energy sources has been on the rise, with solar energy being the most widely adopted. Solar cells, which transform solar energy into electricity, have drawn considerable interest. Traditional silicon-based solar cells, known for being costly and less efficient, are being superseded by dye-sensitized solar cells (DSSCs)<sup>1</sup>. Since Grätzel *et al.* developed dye-sensitized solar cells (DSCs), a new type of solar cells, in 1991, these have attracted considerable attention due to their environmental friendliness and low cost of production<sup>2</sup>. Triphenylamine-based D- $\pi$ -A structure as sensitizer for dye sensitized solar cells attain considerable attention because of their structural versatility, low cost, and high molar absorption coefficient<sup>3</sup>. The overall efficiency of the DSSCs depends on the photosensitizers<sup>4</sup>. Photosensitizers are categorized into metal complex and metal-free organic sensitizers in which metal-free organic photosensitizers are preferred over Ruthenium based

sensitizers because of their low cost and good transport properties<sup>5,6</sup>. The advantages of organic dyes over metal complex sensitizers include higher molar absorption coefficients, the wide variety of molecular structures available and their flexibility for facile molecular design have attracted more emphasis on the research on organic sensitizers based DSSC<sup>7</sup>. Recently, the aromatic  $\pi$ -spacer polycarboxylates ligands have attracted extensive attention because of their brilliant combining properties, including complexation, and the possibility of offering new functional materials<sup>8</sup>. The rationale structural alterations in 1,4-Naphthalene Dicarboxylic Acid based photosensitized dyes were explored to boost the electron injection efficiency of DSSCs. The 1,4-Naphthalene Dicarboxylic Acid (1,4-NDC) ligand as an essential aromatic carboxylic ligand, possessing unique structural features has shown an excellent bridging role, containing the diversity coordination modes from two carboxylate groups with four oxygen atoms, high symmetry and structural rigidity being from rigidity of the naphthalene ring<sup>9</sup>. Moreover, the aromatic carboxylic acid is capable to form  $\pi \cdots \pi$

stacking interactions, which play an important role in the formation of packing structures<sup>10</sup>. Organic sensitizers, D- $\pi$ -A (donor, bridge, and acceptor) groups are often to show and achieve higher effectiveness of intramolecular charge transfer under photo induced conditions<sup>11</sup>. The 1,4-Naphthalene Dicarboxylic Acid derivatives and newly developed sensitizers is displayed in Fig. 1, that generate sufficient D- $\pi$ -A (Fig. 2) are evaluated and reported in the present work. The theoretical analysis



NDC-1	$R_1=CH_3$	$R_2=C_3H_2NO_2$
NDC-2	$R_1=C_2H_5$	$R_2=C_3H_2NO_2$
NDC-3	$R_1=CH_3$	$R_2=C_3H_2CN$
NDC-4	$R_1=C_2H_5$	$R_2=C_3H_2CN$

Fig. 1 — Molecular structure of newly developed dyes

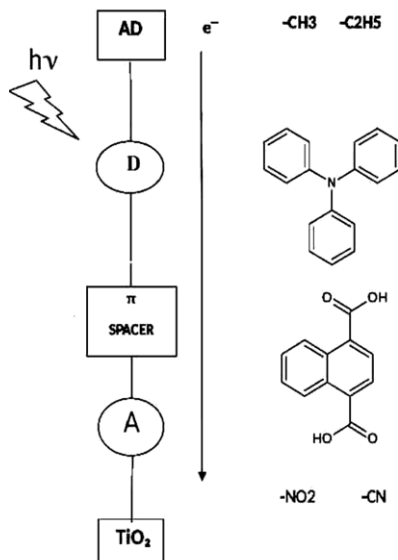


Fig. 2 — Different components of the 1,4-Naphthalene Dicarboxylic Acid AD-D- $\pi$ -A system

of the structural modifications in NDC based photosensitized dyes is to improve the electron injection efficiency of DSSC where a large panel of new structures can be tested and all modifications are theoretically possible. The electrolyte used in DSSC is generally  $I_3^- / I^-$  system. In this investigation, 1,4-Naphthalene Dicarboxylic Acid act as a  $\pi$ -spacer. The donor is a Triphenylamine (TPA) group, while the triphenyl amine group serves as the component that donates electrons in each system, the nitro ( $NO_2$ ) / cyano ( $CN\equiv N$ ) is used as an electron accepting group. An alternate methyl/ethyl group is employed to study the effect of the auxiliary donor group (Fig. 2).

### Theoretical Background

A robust theoretical approach is proposed to accurately determine electron injection into the Titanium Oxide ( $TiO_2$ ) surface from selected 1,4-Naphthalene Dicarboxylic Acid derivatives. This method, based on analyzing the electrochemical characteristics of the dyes in their excited state, reports the change in free energy due to electron injection in electron volts (eV).

$$\Delta G^{inject} = E_{OX}^{dye*} - E_{CB}^{TiO_2} \quad \dots (1)$$

where,  $E_{OX}^{dye*}$  is the oxidation potential energy of the dye in the excited state and  $E_{CB}^{TiO_2}$  is the reduction potential of the conduction band (CB) of the  $TiO_2$  (4.0 eV)<sup>12,13</sup>. The  $E_{OX}^{dye*}$  can be estimated as<sup>14</sup>

$$E_{OX}^{dye*} = E_{OX}^{dye} - \lambda_{max}^{ICT} \quad \dots (2)$$

where  $E_{OX}^{dye}$  is the oxidation potential energy of the dye at the ground state and  $\lambda_{max}^{ICT}$  is the electronic vertical transition energy corresponding to  $\lambda_{max}$  (Fig. 3).

The effectiveness of a DSSC is determined by how efficiently the dyes respond to incident light. To maximize photocurrent generation, the values should closely align with the dyes light harvesting efficiency (LHE). The light harvesting efficiency (LHE) was calculated using the following formula:

$$LHE = 1 - 10^{-f} \quad \dots (3)$$

where  $f$  is the dye's oscillator strength<sup>12</sup>. Since electrons are injected into the conduction band from the LUMO ( $E_{CB}$ ) of the semiconductor  $TiO_2$ , the energy of the dye's LUMO ( $E_{LUMO}$ ) may be utilized to

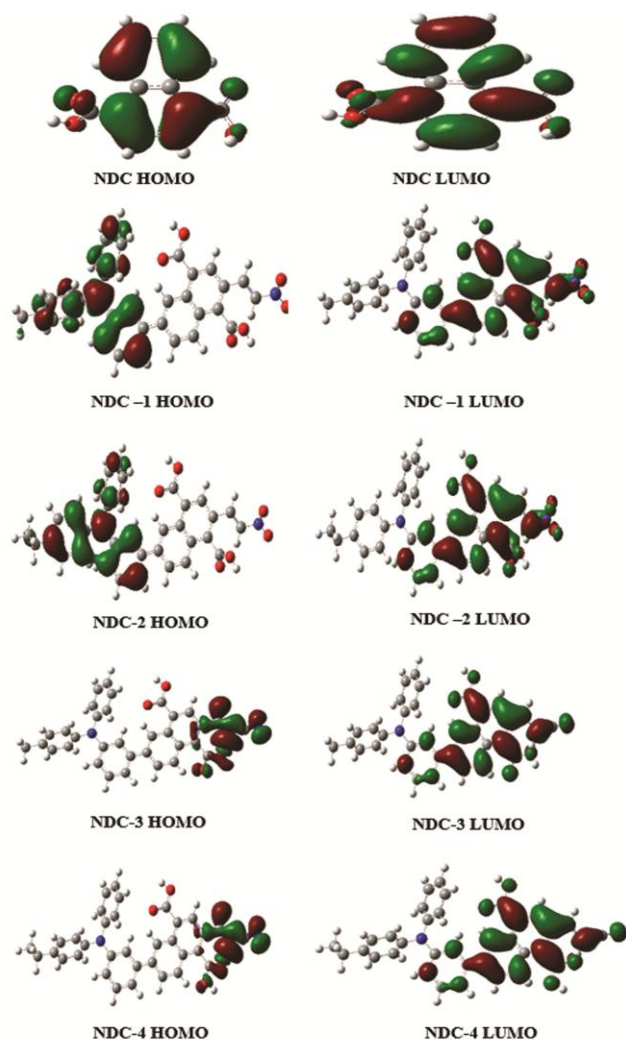


Fig. 3 — HOMO and LUMO distribution pattern of 1,4-Naphthalene Dicarboxylic Acid based dyes in gas phase by DFT/B3LYP/6-311+G(d,p) level of theory

calculate the open circuit photovoltage  $V_{oc}$  (eV)<sup>15</sup> (Fig. 4).

$$V_{oc} = E_{LUMO} - E_{CB} \quad \dots (4)$$

The electron coupling constant  $|V_{RP}|$  is obtained<sup>16</sup> from using eqn. 5.

$$|V_{RP}| = \frac{\Delta G_{inject}}{2} \quad \dots (5)$$

### Computational Method

In the present work, full geometry optimizations and electronic structure calculations of 1,4-Naphthalene dicarboxylic acid (NDC) sensitizers were first performed in vacuum using the B3LYP functional with 6-311 + G (d,p) basis set. To obtain energies comparable to the available experimental results, the ground state geometries of the studied

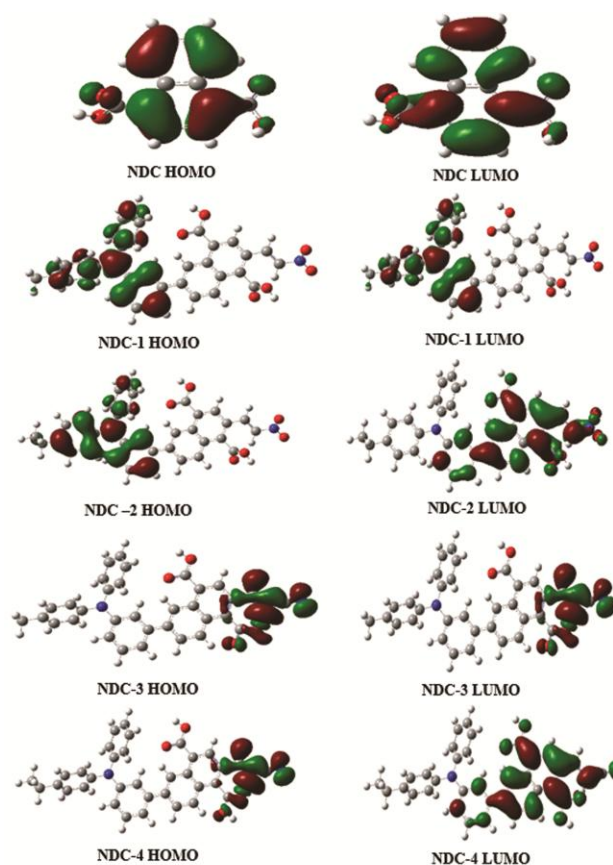


Fig. 4 — HOMO and LUMO distribution pattern of 1,4-Naphthalene Dicarboxylic Acid based dyes in DMF by DFT/B3LYP/6-311+G(d,p) level of theory

NDC sensitizers in the solvent Dimethyl Formamide (DMF) were optimized using the Polarized Continuum Model (PCM) with a larger basis set, 6-311+G(d,p). The package used in the present computation<sup>17</sup> is Gaussian 09. Density functional theory with Becke's three parameters functional and the Lee-Yang-Parr functional (B3LYP) was employed in the structural optimization of the ground state of the dyes in the gas phase with 6-311+G(d, p) basis set<sup>18-20</sup>.

## Results and Discussion

### Molecular Orbitals

Molecular orbital (MO) analysis at the B3LYP/6-311+G(d,p) level of theory was conducted to gain deeper insights into the molecular structure and electronic distribution of these dyes. The optimized structures of all the organic dyes show a similar coplanar conformation. This coplanar structure is expected to enhance electron transfer from the electron donor to the electron acceptor through the  $\pi$ -

spacer unit in these dyes. A key feature of organic sensitizers is the intramolecular charge transfer (ICT) from the donor to the acceptor or anchoring groups. The ICT behavior was analyzed using the contributions of the Frontier molecular orbitals (FMO). The spatial distributions of the HOMO and LUMO orbitals for all dyes were analyzed, revealing typical  $\pi$ -type characteristics. HOMOs exhibited anti-bonding between adjacent fragments and bonding within units, while LUMOs showed bonding between fragments. The electron distributions showed that HOMOs are mainly located in the donor and  $\pi$ -conjugated spacer, and LUMOs are focused on the  $\pi$ -conjugated spacer and acceptor fragments. This configuration allows for intramolecular charge transfer (ICT) from the donor to the acceptor through the conjugated bridge, classifying the HOMO-LUMO transition as  $\pi$ - $\pi^*$  ICT.

To gain a deeper understanding of how electronic properties depend on molecular structure, the analysis focused on the energy levels of the Frontier molecular orbitals (HOMO and LUMO) and the energy gap ( $E_g$ ) of these dyes, as shown in Fig. 5 and Fig. 6. The electron-donating ability of the donor groups in D- $\pi$ -A dyes influences their electrochemical properties. A dye with a stronger electron donor group tends to have a higher HOMO level compared to one with a weaker donor. Table 1 lists the effects of different donor groups on electronic properties, showing that the HOMO values are highest for NDC-4 and lowest for NDC. The NDC-4 dye, with the strongest electron donor group, has the highest HOMO level (-4.5302

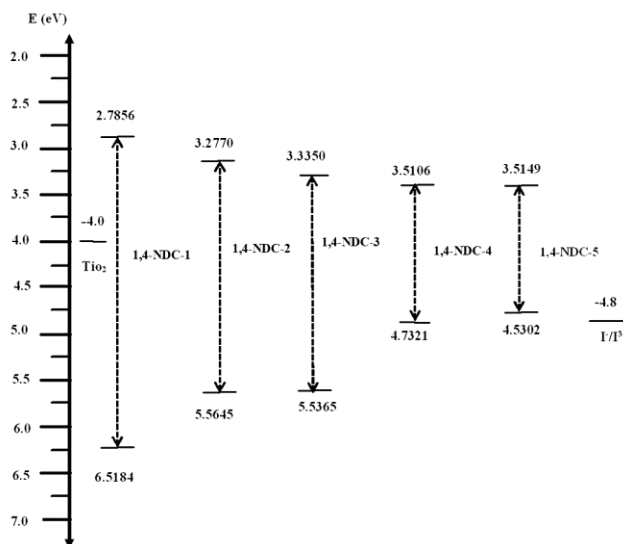


Fig. 5 — Energy level diagram ( $E_{\text{HOMO}}$  and  $E_{\text{LUMO}}$ ) of the 1,4-Naphthalene Dicarboxylic Acid based dyes in gas phase

eV), while the parent dye, lacking donor or acceptor groups, has a weaker electron donation capability. Fig. 5 and Fig. 6 also indicate that the LUMO levels of all sensitizers are relatively stable across different molecular structures, as the inclusion of electron acceptor groups has less impact compared to changes in the donor groups. The LUMO energy levels of all the dyes are much higher than that of  $\text{TiO}_2$  conduction band<sup>21</sup>. Moreover, the molecules in excited state have a strong ability to eject electrons into  $\text{TiO}_2$  electrodes. The HOMO of dyes NDC-3 and NDC-4 is lower than that of -4.8 eV<sup>22</sup>. Therefore, these molecules that lose electrons could be restored by getting electrons from electrolytes. Thus, electron injection of the excited molecules and subsequently regeneration of oxidized species is energetically permitted. This allows the application of dyes in DSSC. The energy gap for studied molecules was obtained by the difference of HOMO and LUMO energy levels and are listed in Table 1.

The order of energy gap is: NDC > NDC-1 > NDC-2 > NDC-3 > NDC-4. When the energy gap decreases, more photons at the longer wavelength side would be absorbed to excite the electrons into the unoccupied molecular orbital which increases short circuit current density and further enhances the efficiency. From the values of energy gap, we decided that these dyes have the potential to be employed in the DSSC application. For spontaneous charge regeneration to occur, the energy level of the highest occupied molecular orbital

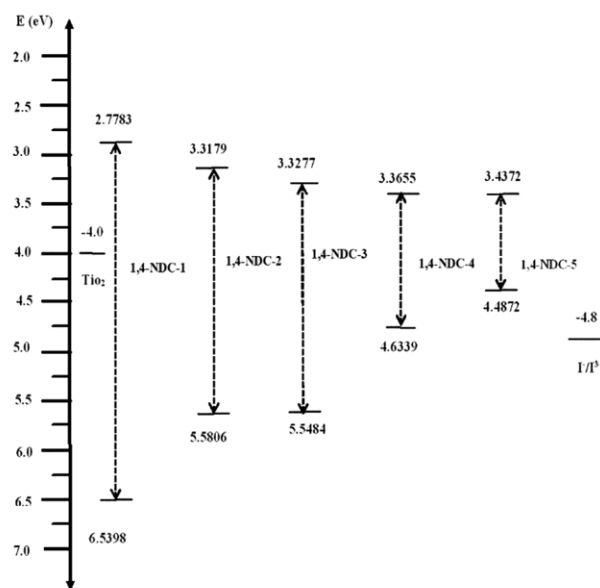


Fig. 6 — Energy level diagram ( $E_{\text{HOMO}}$  and  $E_{\text{LUMO}}$ ) of the 1,4-Naphthalene Dicarboxylic Acid based dyes in DMF

Table 1 — Calculated  $E_{\text{HOMO}}$ ,  $E_{\text{LUMO}}$  and energy gap ( $E_g$ ) of 1,4-Naphthalene Dicarboxylic Acid dyes in eV at B3LYP/6-311+G (d, p) level of theory

Dye	Gas Phase			DMF		
	$E_{\text{HOMO}}$	$E_{\text{LUMO}}$	$E_{\text{GAP}}$	$E_{\text{HOMO}}$	$E_{\text{LUMO}}$	$E_{\text{GAP}}$
NDC	-6.5184	-2.7856	3.75	-6.5398	-2.7783	3.76
NDC-1	-5.5645	-3.2770	2.29	-5.5806	-3.3179	2.26
NDC-2	-5.5365	-3.3350	2.20	-5.5484	-3.3277	2.22
NDC-3	-4.7321	-3.5106	1.22	-4.6339	-3.3655	1.27
NDC-4	-4.5302	-3.5149	1.02	-4.4872	-3.4371	1.05

Table 2 — Calculated absorption maxima ( $\lambda_{\text{max}}$ ),  $\Delta G^{\text{inject}}$ , oxidation potential, intermolecular charge transfer for energy of dyes at TDDFT/CAM – B3LYP16-311+G(d,p) level of theory

Dye	Gas Phase					DMF				
	$\lambda_{\text{max}}$	$\Delta G^{\text{inject}}$	$E_{\text{OX}}^{\text{dye}}$ *	$E_{\text{OX}}^{\text{dye}}$	$\lambda_{\text{max}}^{\text{ICT}}$	$\lambda_{\text{max}}$	$\Delta G^{\text{inject}}$	$E_{\text{OX}}^{\text{dye}}$ *	$E_{\text{OX}}^{\text{dye}}$	$\lambda_{\text{max}}^{\text{ICT}}$
NDC	380	-0.7442	3.2578	6.5185	3.2607	379	-0.7316	3.2684	6.5398	3.2714
NDC-1	499	-0.9187	3.0813	5.5645	2.4832	505	-0.8747	3.1253	5.5806	2.4553
NDC-2	501	-0.9392	3.0608	5.5365	2.4757	507	-0.8946	3.1054	5.5484	2.4430
NDC-3	761	-0.8974	3.1026	4.7321	1.6295	683	-1.1813	2.8187	4.6339	1.8152
NDC-4	765	-1.0903	2.9097	4.5302	1.6205	705	-1.2723	2.7277	4.4872	1.7595

(HOMO) must be more negative than the reduction potential of the electrolyte ( $\text{I}_3^-/\text{I}^-$ ), which is  $-4.80$  eV. Additionally, for spontaneous charge transfer from the dye-excited state to the  $\text{TiO}_2$  conduction band, the energy level of the lowest unoccupied molecular orbital (LUMO) must exceed the  $\text{TiO}_2$  potential of  $-4.0$  eV. By using the polarizable continuum model, the HOMO and LUMO energy levels of the dyes were assessed in both the gas phase and in DMF. The LUMO levels of the dyes are generally higher than the  $\text{TiO}_2$  conduction band energy, while the HOMO levels are slightly below the electrolyte's redox potential. This confirms that the dyes are compatible with  $\text{TiO}_2$  for effective spontaneous charge transfer and regeneration.

### Optical properties

To gain insights of the optical property and electronic transition, the excitation energy and UV-VIS absorption spectra for the singlet-singlet transition of all sensitized dyes were simulated using TDDFT with B3LYP functional in gas and in DMF solution<sup>22,23</sup>. Previous studies utilized DMF as the solvent for UV-VIS absorption spectra of NDC-based molecules<sup>24-27</sup>. Table 2 lists the computed vertical excited singlet states and transition energies of all sensitized dyes in both vacuum and solvent media. The simulated absorption spectra of these compounds, obtained using the PCM/B3LYP/6-311+G(d,p) level of theory, are depicted in Fig. 7 and Fig. 8. The spectra exhibit a similar profile for all dyes, with a prominent intense band between 455 and 500 nm.

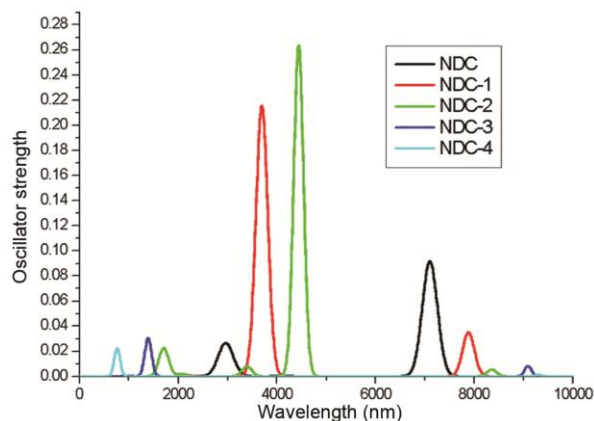


Fig. 7 — Simulated absorption spectra of dyes calculated in Gas Phase at TDDFT / B3LYP/6-311+G(d,p) level of theory

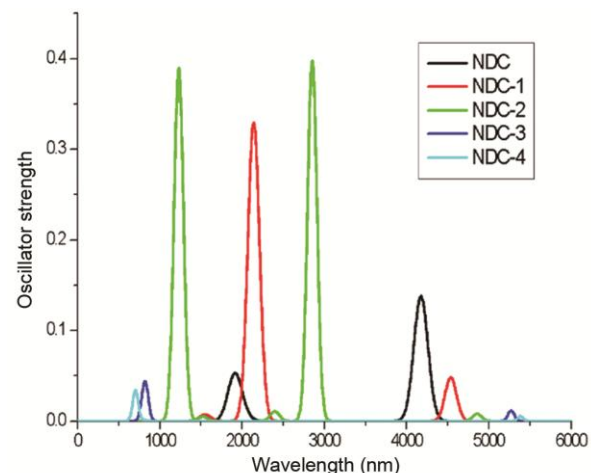


Fig. 8 — Simulated absorption spectra of dyes calculated in DMF at TDDFT / B3LYP/6-311+G(d,p) level of theory

Table 3 — Excitation Energy (E), Light Harvesting Efficiency (LHE), and average Light Harvesting Efficiency ( $LHE_{Average}$ ) of dyes at TDDFT/CAM-BBLYP/6-311+G(d,p) level of theory

Dye	Gas Phase				DMF			
	E (eV)	$\lambda$ (nm)	LHE	$LHE_{Avg}$	E(eV)	$\lambda$ (nm)	LHE	$LHE_{Avg}$
NDC	3.2607	380	0.1898	0.1245	3.2714	379	0.2723	0.1927
	3.9406	315	0.0592		3.9321	315	0.1132	
NDC-1	2.4832	499	0.3912	0.2343	2.4553	505	0.5315	0.3129
	1.9289	643	0.0774		1.9218	645	0.0943	
NDC-2	2.4757	501	0.4552	0.2367	2.4430	507	0.6000	0.5961
	2.7200	456	0.0182		3.1974	388	0.5923	
NDC-3	1.6295	761	0.0676	0.0344	1.8152	683	0.0905	0.0488
	1.8882	657	0.0012		1.7938	691	0.0071	
NDC-4	1.6205	765	0.0478	0.0252	1.7595	705	0.0753	0.0388
	1.5812	784	0.0025		1.5072	823	0.0023	

Table 4 — Electron coupling constants ( $|V_{RP}|$ ) and open-circuit voltage ( $V_{oc}$ ) of NDC based dyes

Dye	Gas Phase		DMF	
	$V_{RP}$	$V_{oc}$	$V_{RP}$	$V_{oc}$
NDC	0.37	1.21	0.36	1.22
NDC-1	0.46	0.72	0.44	0.68
NDC-2	0.47	0.66	0.45	0.67
NDC-3	0.45	0.49	0.59	0.63
NDC-4	0.54	0.48	0.64	0.56

This main band predominantly results from excitation from the HOMO to the LUMO orbital in both gas and solvent phases. Fig. 7 and Fig. 8 show the UV-VIS absorption spectra of NDC and the newly designed dyes. All dyes experience a red shift in DMF, with NDC-2, NDC-3, and NDC-4 showing a more pronounced red shift compared to NDC and NDC-1 in the gas phase. The solvent effect on NDC's absorption spectrum is minimal (314nm to 315 nm). The red shift follows the order: NDC-4 > NDC-3 > NDC-2 > NDC-1 > NDC, which is inversely related to the HOMO-LUMO energy gap. Dyes with a smaller energy gap require less energy for electronic transitions, leading to longer absorption wavelengths.

The absorption spectra of NDC-3 and NDC-4 also indicate absorption in the near-infrared and visible regions. So, we can say that dye will work in dim light by the absorption of infrared radiation. This dye is also environment friendly because it absorbs the infrared radiation which causes global warming. On the other hand, the dye NDC-1 and NDC-2 absorb in visible region. The LHE is the efficiency of dye to respond to light. It is another factor which indicates the efficiency of DSSC and it maximizes the photo current regions, the calculated LHE of absorption peaks of NDC and newly designed dyes are shown in Table 3. From the Table 3, NDC-2 will give more LHE in gas phase as well as in solvent medium than

that of the other dyes studied here. The dyes NDC-1 and NDC-2 will convert more light to electrical energy. The open circuit ( $V_{oc}$ ) is another important property in designing DSSCs. Table 4 contains the  $V_{oc}$  values of the dyes. It can be seen from the data in Table 4 that the potential value is close to 1 eV in the NDC derivative based DSSCs. This shows that the NDC derivatives are potential candidates in the design of DSSCs. The coupling constant ( $|V_{RP}|$ ), is a factor that affects the rate of electron injection between the organic dyes and the semiconductor surface. This can be calculated using equation 5. Higher the electron-coupling constant faster is the rate of electron injection. The computed values of  $V_{RP}$  are listed in Table 4 for the investigated dyes. Recently, Irfan *et al.* investigated structure modification to tune electronic and charge transfer properties of solar cell materials using DFT method and found that when more activating group is present in donor part and more deactivating group is present in acceptor part of the sensitizer,  $\Delta G^{inject}$  and  $V_{RP}$  are increased<sup>28</sup>. In the present study it is observed that NDC-4 and NDC-3 have high  $V_{RP}$  values since they contain the -CN group in the acceptor part.

## Conclusion

The electronic structure and optical absorption properties of NDC and newly designed dye sensitizers

were analyzed using Density Functional Theory. The study examined how different electron donor groups affect the electronic structure and optical properties. It also investigated the impact of these donor groups on the open circuit voltage ( $V_{oc}$ ) and electron coupling constant ( $|V_{RP}|$ ), to identify suitable sensitizers for DSSCs. The results indicate that the NDC dyes exhibit favorable photo-physical properties for DSSC applications, with NDC-2, featuring a  $C_2H_5$  donor group, emerging as the best sensitizer. NDC-2 shows optimal oxidation potential energies, high open circuit voltage, and effective electron injection into the  $TiO_2$  conduction band, making it a strong candidate for DSSC applications.

### References

- Mahmood A, *Solar Ene Rev*, 123 (2016) 127.
- O'regan B & Gratzel M, *Nature*, 353 (1991) 737.
- Narayanaswamy K, Swetha T, Kapil G, Pandey S S, Hayase S & Singh S K, *Electrochim Acta*, 169 (2015) 256.
- Zhou H, Wu L, Gao Y & Ma T, *J Photochem Photobio Chem*, 219 (2011) 188.
- Du W, Li H B, Geng Y, Wu Y, Zhang M, Su Z M, *J Photochem Photobio*, 301 (2015) 40.
- Liu Y, Li J, Liu D, Li X, Xu Y, *J Comp Mat Sci*, 161 (2019) 163.
- Guillen A S E, Kavan L, Gratzel M & Naseeruddin M K, *Energy Env Sci*, 6 (2013) 3439.
- Mehmood U, Ibbelwaleed A, Daud H M, Ahmed S & Khalil H, *Dyes Pigments*, 118 (2015) 152.
- Xing Y, Liu Y, Xue X, Wang X & Li W, *J Mol Str*, 1154 (2018) 547.
- Wang H, Deng X C & Dong G-Y, *Inorganica Chim Acta*, 558 (2023) 121731.
- Krishnaveni S, Mary J X, Mohan K S & Sathyanarayanamoorthi V, *Asian J Chem*, 35 (2023) 2215.
- Katoh R, Furube A, Yoshihara T, Hara K, Fujihashi G, Takano S, Murata S, Arakawa H & Tachiya M J, *J Phys Chem B*, 108 (2004) 4818.
- Asbury J B, Wang Y Q, Hao E, Ghosh H N & Lian T, *Res Chem Intermed*, 27 (2001) 393.
- Hagfeldt A & Gratzel M, *Chem Rev*, 95 (1995) 49.
- Zhang Z G, Min J, Zhang S, Zhang J, Zhang M & Li Y, *Chem Comm*, 47 (2011) 9474.
- Odey J O, Louis H, Agwupuye J A, Moshood Y L, Bisong E A & Brown O I, *J Mol Struct*, 1241 (2021) 130615.
- Barbe C J, Arendse F, Comte P, Jirousek M, Lenzmann F, Shklover V & Gratzel M, *J Ame Chem Soc*, 803 (2015) 157.
- Shanmugam M, Durcan C & Gedrim R, 2 (2013) 523.
- Gratzel M & Zakeeruddin S, *Mat Today*, 16 (2013) 11.
- Li D M, Qin D & Deng M H, *Energy Env Sci*, 2 (2009) 283.
- Asbury J B, Wang Y Q, Hai E, Ghosh H, Lian T, *Res Chem Int*, 27 (2001) 393.
- Hagfeldt A & Gratzel M, *Chem Rev*, 95 (1995) 49.
- Jacquemin D, Perpete E A & Ciofinil C, *Adamo Acc Chem Res*, 42 (2009) 326.
- Adamo C & Jacquemin D, *Chem Soc Rev*, 42 (2013) 845.
- Ando S, Nishida J, Inohue Y, Tokito S & Yamashita Y, *J Mater Chem*, 14 (2004) 1787.
- Hu C, Wu Z, Cao K, Sun B & Zhang Q, *Polymer*, 54 (2013) 1098.
- Cheng P, Shi Q, Lin Y, Li Y & Zhan X, *Org Electron*, 14 (2013) 599.
- Irfan A, Mohammad S, Abdullah A-S & Mohammad S A-A, *Int J Electrochem Sci*, 10 (2015) 3600.